hPOC5 is a centrin-binding protein required for assembly of full-length centrioles

Juliette Azimzadeh,[1] Polla Hergert,[2] Annie Delouvée,[1] Ursula Euteneuer,[3] Etienne Formstecher,[4] Alexey Khodjakov,[2] and Michel Bornens[1]

[1]Institut Curie, Centre National de la Recherche Scientifique Unité Mixte de Recherche 144, 75248 Paris, Cedex 05, France
[2]Wadsworth Center, New York State Department of Health, Albany, NY 12201
[3]Adolf-Butenandt-Institute, Cell Biology, Ludwig Maximilian University of Munich, 80336 Munich, Germany
[4]Hybrigenics, 75014 Paris, France

Centrin has been shown to be involved in centrosome biogenesis in a variety of eukaryotes. In this study, we characterize hPOC5, a conserved centrin-binding protein that contains Sfi1p-like repeats. hPOC5 is localized, like centrin, in the distal portion of human centrioles. hPOC5 recruitment to procentrioles occurs during G2/M, a process that continues up to the full maturation of the centriole during the next cell cycle and is correlated with hyperphosphorylation of the protein. In the absence of hPOC5, RPE1 cells arrest in G1 phase, whereas HeLa cells show an extended S phase followed by cell death. We show that hPOC5 is not required for the initiation of procentriole assembly but is essential for building the distal half of centrioles. Interestingly, the hPOC5 family reveals an evolutionary divergence between vertebrates and organisms like *Drosophila melanogaster* or *Caenorhabditis elegans*, in which the loss of hPOC5 may correlate with the conspicuous differences in centriolar structure.

Introduction

In animal cells, the duplication of the centrosome and its structural stability depend on centrioles (Sluder and Rieder, 1985; Bobinnec et al., 1998). Centrioles, or basal bodies, are found in a wide variety of eukaryotic species and probably originate in a common ancestor (Baroin et al., 1988).

In human cells, centrioles display a structural polarity, with stable triplet microtubules at their proximal end and doublet microtubules at their distal end (Paintrand et al., 1992; Rousselet et al., 2001). In addition, mature centrioles harbor two sets of appendages at their distal ends, which are thought to be required for anchoring microtubules at the centriole, and for docking centrioles at the plasma membrane during ciliogenesis (Piel et al., 2000; Ishikawa et al., 2005).

During G1 phase of the cell cycle, the centrosome contains a mature centriole, referred to as the mother centriole, and an immature centriole assembled during the previous cell cycle, referred to as the daughter centriole. Centriole duplication is first seen during S phase by the appearance of procentrioles that form at right angles to the proximal ends of preexisting centrioles (Robbins and Gonatas, 1964; Robbins et al., 1968; Kuriyama and Borisy, 1981; Vorobjev and Chentsov Yu, 1982). Procentrioles elongate as the cell cycle progresses to reach nearly full length in mitosis. During prophase, the two new centrosomes, each containing a parental and a newly formed centriole, migrate apart and organize the mitotic spindle. Procentrioles become daughter centrioles after mitosis, and it is only after a second mitosis that these centrioles become fully mature mother centrioles, bearing the two sets of distal appendages (Vorobjev and Chentsov Yu, 1982). Thus, centriole assembly and the maturation cycle encompass three successive cell cycles.

In the past few years, numerous data obtained from diverse model organisms have allowed us to draw a much clearer picture of the mechanisms governing the initial steps of centriole duplication (for review see Bettencourt-Dias and Glover, 2007). However, the fine structural changes and the associated molecular mechanisms that underlie centriole elongation and maturation remain poorly understood.

Correspondence to Michel Bornens: michel.bornens@curie.fr

J. Azimzadeh's present address is Biochemistry and Biophysics Dept., University of California, San Francisco, San Francisco, CA 94143.

Abbreviations used in this paper: CBR, centrin-binding repeat; HU, hydroxyurea; PCNA, proliferating cell nuclear antigen.

The Rockefeller University Press $30.00
J. Cell Biol. Vol. 185 No. 1 101–114
www.jcb.org/cgi/doi/10.1083/jcb.200808082

In most eukaryotes, members of the centrin family are found associated with the centrioles, basal bodies, and associated structures. Centrin proteins have several specific locations within centrioles/basal bodies and axonemes (Levy et al., 1996; Paoletti et al., 1996; Laoukili et al., 2000; Lemullois et al., 2004; Geimer and Melkonian, 2005; Ruiz et al., 2005; Stemm-Wolf et al., 2005) and are also components of various fiber systems associated with basal bodies in a spectrum of organisms (Salisbury et al., 1988; Madeddu et al., 1996). In human cells, the ubiquitous centrin proteins hCen2 and hCen3 are recruited very early to assembly sites of procentrioles and are found within the distal lumen of full-length centrioles (Paoletti et al., 1996; Middendorp et al., 1997; Laoukili et al., 2000). Centrin proteins have been proposed to play a role in centriole assembly, as knockout of the *Tetrahymena thermophila* or *Chlamydomonas reinhardtii* homologues of hCen2 prevents centriole/basal body duplication (Koblenz et al., 2003; Stemm-Wolf et al., 2005), although a similar requirement for centrin proteins in mammalian centrosome duplication remains controversial (Salisbury et al., 2002; Kleylein-Sohn et al., 2007). This function could also be conserved in higher fungi, although centriolar structure is lost in this lineage during evolution (Adams and Kilmartin, 2000). The budding yeast centrin Cdc31p and its homologue in fission yeast are indeed required for the duplication of spindle pole bodies, which are the acentriolar centrosomes of fungi (Baum et al., 1986; Paoletti et al., 2003).

Despite their evolutionary conservation and their common association with centriolar structures, the precise functions of centrin proteins await characterization. Like CaM, to which they are closely related, centrin proteins could interact with several partners to ensure flagellar apparatus or centrosome-associated functions as well as other apparently unrelated processes such as DNA repair and mRNA export (Araki et al., 2001; Fischer et al., 2004; Nishi et al., 2005). A conserved centrin-interacting protein associated with centrosomes, Sfi1p, has been first identified in yeast. Like Cdc31p, Sfi1p is essential for spindle pole body duplication, and its human homologue localizes to the centrioles in human cells (Kilmartin, 2003).

In this study, we report the characterization of a novel, conserved centrin-binding protein containing centrin-binding repeats (CBRs) similar to those found in Sfi1p. This protein, which we called hPOC5, is concentrated at the distal end of centrioles. We show that hPOC5 is not required for initial procentriole formation but is required for the assembly of the distal portion of centrioles and progression into G2 phase of the cell cycle.

Results

Identification of hPOC5, an evolutionarily conserved centrin-binding protein

We have used a two-hybrid approach to identify proteins interacting with human centrin proteins hCen2 or hCen3. Screening human two-hybrid libraries using full-length or a C-terminal region (aa 93–173) of hCen2 led to the identification of five partial cDNA clones corresponding to the same region of the GenBank/EMBL/DDBJ (NM_001099271) mRNA sequence. It encodes the C5orf37/FLJ35779 protein, which has been found to be a putative component of human centrosomes by mass spectrometry analysis (Andersen et al., 2003). A candidate *C. reinhardtii* homologue called POC5 (proteome of centriole 5) has also been found in centriole fractions (Keller et al., 2005). Therefore, we called the human protein hPOC5.

A full-length cDNA encoding the 575-aa hPOC5 protein was cloned by RT-PCR from HeLa RNA extracts. The amino acid sequence of hPOC5 predicted three putative Sfi1p-like CBRs. Two of them defined a tandem repeat after the consensus sequence $[F/W/L]X_2W[R/K]X_{21\text{-}34}[F/W/L]X_2W[R/K]$ found in Sfi1 protein family members (Fig. 1, a and b; Kilmartin, 2003; Li et al., 2006). In addition, two short coiled-coil domains are predicted on both sides of the tandem repeat.

Homologues of hPOC5 are found in many eukaryotic species, including vertebrates, the green algae *C. reinhardtii,* and the protists *Trypanosoma brucei*, *Leishmania major*, *Giardia lamblia*, and *Paramecium tetraurelia* (Fig. 1, b and c), indicating a very ancient origin. Overall sequence conservation between POC5 family members is moderate (mean 16% identity and 29% similarity between distantly related species) with the exception of a very conserved sequence of 21 aa (mean 57% identity and 81% similarity). All of the potential hPOC5 homologues contain the tandem repeat of centrin-binding sequences and the short coiled-coil regions. Potential homologues of hPOC5 are not found in the genomes of *Saccharomyces cerevisiae* and *Dictyostelium discoideum*, which do not assemble centrioles; they are also absent in the malarial parasite *Plasmodium falciparum*, in insects, and in nematodes.

hPOC5 binds human centrin proteins

It has been shown that the CBRs of hSfi1 protein bind in a similar manner to the different mammalian centrin proteins (Kilmartin, 2003). We wanted to confirm the interaction between hPOC5 and hCen2 and determine whether it also binds to hCen3, which belongs to another centrin subfamily (Azimzadeh and Bornens, 2004). To this end, we have used GST pull-down experiments. The sequence of hPOC5 was first divided into three parts (F1–3; Fig. 2 a), which were then fused to GST and coexpressed with untagged hCen2 or hCen3 in *Escherichia coli*. Only the F2 fragment, which contains the putative CBRs, was able to pull down either hCen2 or hCen3 (Fig. 2 b). To analyze the binding of centrin proteins further, F2 subdomains containing the first CBR (CBR_1) or the tandem repeat (CBR_{2+3}; Fig. 2 a) were fused to GST and incubated with 5 µM purified hCen2, hCen3, or human CaM. In these experiments, CBR_1 was not able to bind centrin proteins (Fig. 2 c). In contrast, CBR_{2+3} bound hCen2 and hCen3 but not CaM. The results presented in Fig. 2 were obtained in low-Ca concentrations (10 mM EGTA), but similar results were obtained using Ca-containing buffers (5 mM $CaCl_2$; not depicted). Thus, the hPOC5 protein is able to directly bind both hCen2 and hCen3 proteins in a Ca-independent manner through the region containing the two evolutionarily conserved centrin-binding motifs. The interaction between hPOC5 and centrin proteins appears to be specific, as hPOC5 does not bind CaM, which is a protein closely related to centrin.

To determine whether these interactions occur in vivo, we performed immunoprecipitation experiments using affinity-purified anti-hPOC5 polyclonal antibodies (Fig. 2 e). These

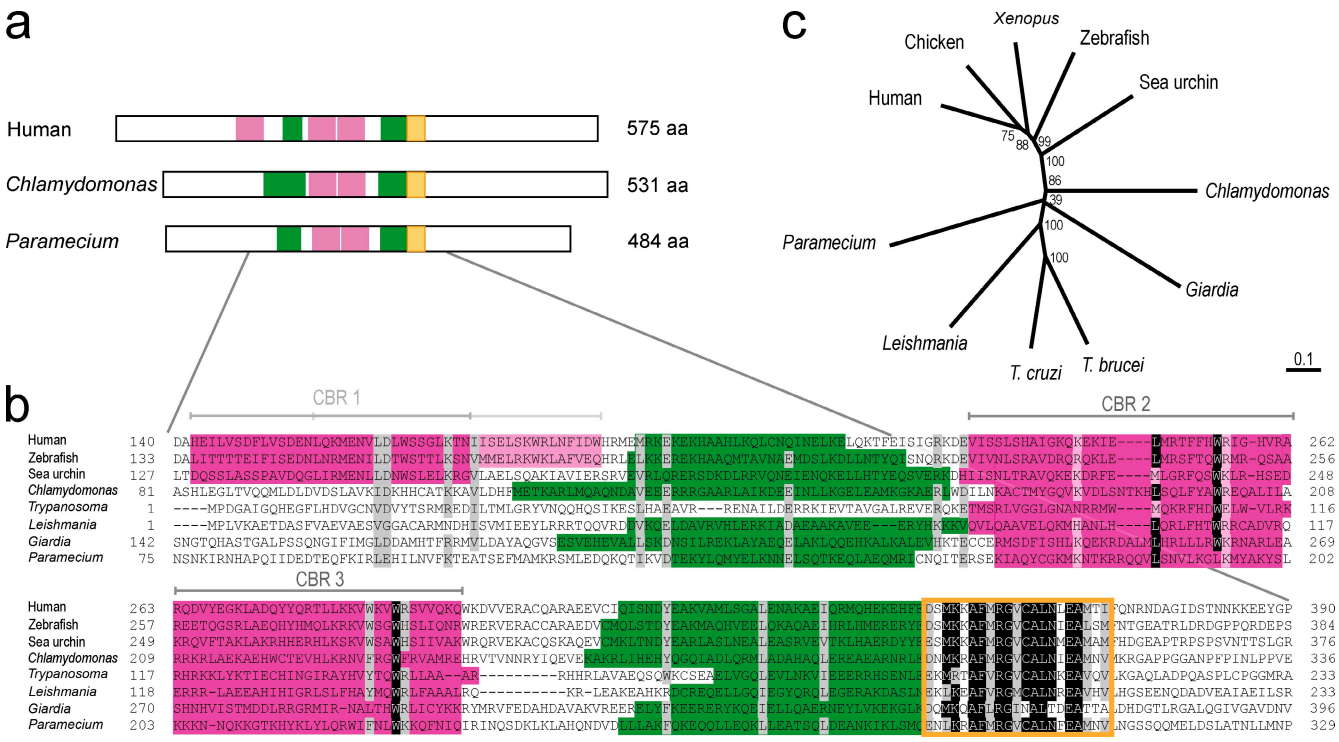

Figure 1. **hPOC5 is a conserved protein.** (a) Schematic representation of hPOC5 and predicted homologues in *C. reinhardtii* and *P. tetraurelia*. The putative Sfi1p-like CBRs are indicated in pink, the predicted coiled-coil regions are indicated in green, and the conserved 21-aa signature domain indicated in orange. The size of the predicted full-length proteins is indicated. (b) Alignment of the central region of POC5 family members: human (available from GenBank/EMBL/DDBJ under accession no. NP_001092741), zebrafish (XP_691080), sea urchin (XP_797483), *T. brucei* (XP_822994), *L. major* (XP_001686847), *G. lamblia* (XP_001705095.1), *C. reinhardtii* (version 3.0 available from the Chlamydomonas Center under accession no. 144089), and *P. tetraurelia* (available from the Paramecium Database under accession no. GSPATP000299360001). Positions at which ≥75% of amino acid residues are identical or similar between proteins are shaded. Identical residues are shaded in black, and similar residues are shaded in gray. Domains depicted in panel a are reported using the same colors on the protein sequences. (c) ClustalW phylogenetic tree of the POC5 family based on the neighbor-joining method. 1,000 replicates were performed. Bootstrap values are displayed as percentages at each node. Bar, 0.1 substitutions/1 aa.

antibodies react predominantly with a doublet of bands in lysates from HeLa cells and with bands of slightly higher molecular weight in insoluble fractions (Fig. 2, d and e). The doublet of bands migrated at ≥75 kD, which is higher than the predicted size (65 kD). The intensity of the major bands was reduced both in lysates and in insoluble fractions after RNAi treatment, indicating that they corresponded to hPOC5 (Fig. 2 d). Anti-hPOC5 antibodies immunoprecipitated endogenous hCen2 and hCen3 from lysates (Fig. 2 e). The reverse coimmunoprecipitation assay showed that hPOC5 coprecipitated either with hCen2 or hCen3. These data suggest that hPOC5 is associated with both hCen2 and hCen3 in vivo.

hPOC5 is a centriolar protein

In immunofluorescence microscopy, anti-hPOC5 antibodies preferentially labeled two dots in interphase cells (Fig. 3 a). These dots corresponded to individual centrioles, as judged by colocalization with GFP-hCen1 (Fig. 3 b). Centriolar localization was also confirmed by expression of full-length hPOC5 fused to GFP (unpublished data). hPOC5 localized at mother and daughter centrioles throughout the cell cycle (Fig. 3 b). The recruitment of centrin proteins in the procentrioles occurs during early S phase (Paoletti et al., 1996; Middendorp et al., 1997; Piel et al., 2000). In contrast, anti-hPOC5 staining of the procentrioles was detected from G2 phase only. It was then seen in increasing amounts as cells progressed through mitosis and the following interphase (Fig. 3 b). As shown in Fig. 3 c, hPOC5 staining was not affected by the complete disassembly of microtubules obtained with nocodazole treatment, indicating that hPOC5 associated with the centrioles in a microtubule-independent manner.

To confirm the predominant localization of hPOC5 at centrosomes, we performed a cellular fractionation analysis (Fig. 3 d). hPOC5 protein was enriched in fractions containing nuclei and centrosomes and enriched even further in isolated centrosomes. Enrichment in hPOC5 was more pronounced in the lymphoid cell line KE37 than in HeLa cells as the result of better centrosome isolation in the former cell line. However, with both cell types, centrosome fractions were enriched in slow migrating forms of hPOC5. We tested whether the electrophoretic pattern was caused by the phosphorylation of hPOC5 (Fig. 3 e). Nuclei and centrosome fractions from HeLa cells incubated with λ-phosphatase only displayed two bands co-migrating with the two prominent soluble forms (Fig. 3 e, left). This suggests that hPOC5 is subject to multiple phosphorylation events upon recruitment in centrioles. To determine whether phosphorylation of hPOC5 was cell cycle dependent, we analyzed the migration pattern of hPOC5 in interphase or mitotic HeLa cell extracts (Fig. 3 e, right). The migration pattern did not vary as cells progressed through G1, S, and G2 phases (unpublished data). However, in mitotic extracts, migration of the two soluble isoforms was shifted toward higher

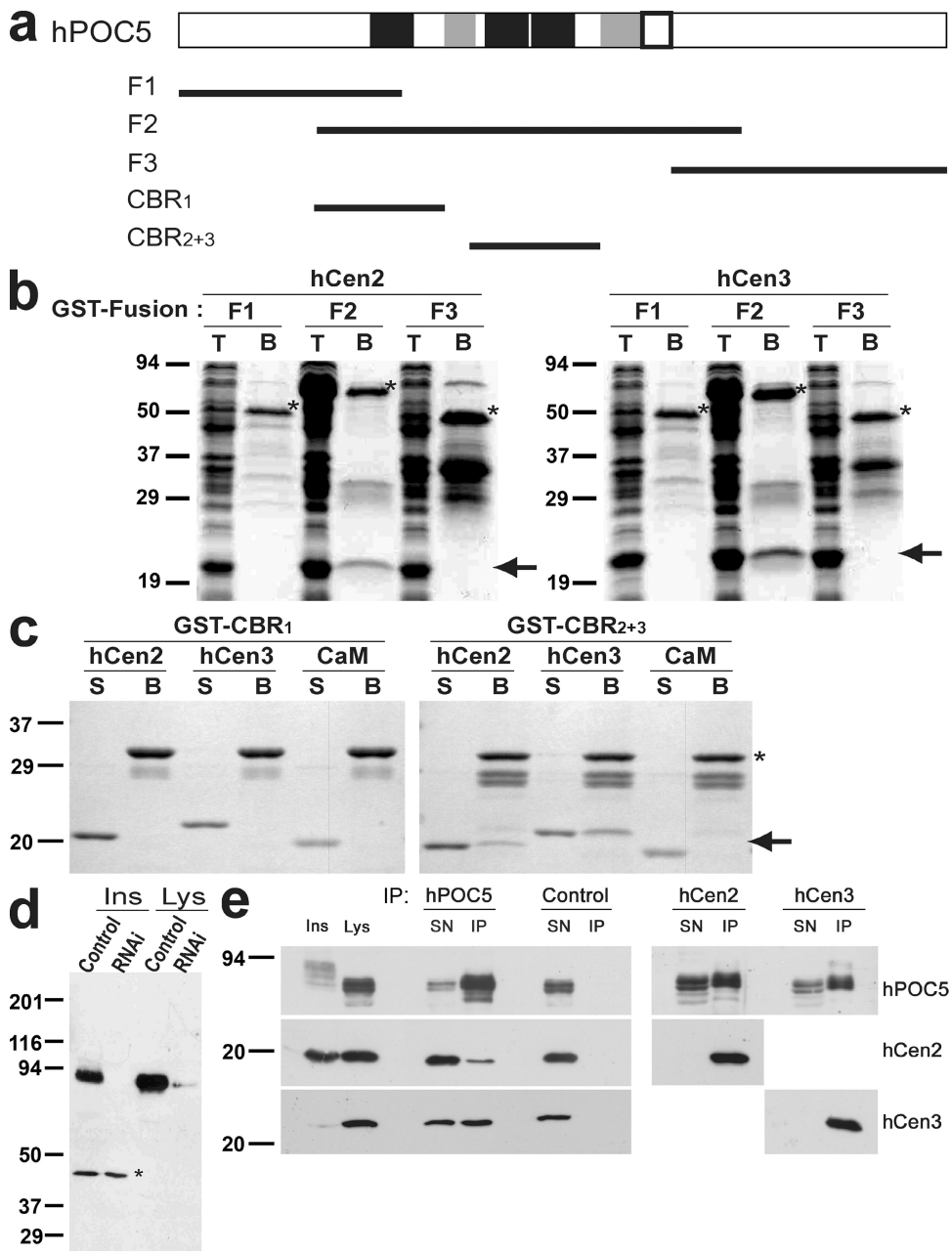

Figure 2. **hPOC5 binds human centrin proteins through the conserved Sfi1p-like repeats.** (a) Maps of the GST fusions used in b and c on a schematic representation of hPOC5 in which CBRs are shown in black, coiled-coil domains are shown in gray, and the POC5 signature domain is outlined in black. (b) GST fusions F1–3 were coexpressed in *E. coli* with hCen2 or hCen3 and pulled down using glutathione beads. T, total *E.coli* extract; B, beads. (c) Fusions containing only the first predicted CBR (CBR_1) or the central conserved tandem repeat (CBR_{2+3}) were bound to glutathione beads and incubated with 5 µM untagged hCen2, hCen3, or CaM. S, supernatant after the pull-down. In b and c, the GST fusions are indicated by an asterisk, and hCen2/3 or CaM is indicated by an arrow. (d) Affinity-purified anti-hPOC5 labels a major band in HeLa cell lysates that can be further resolved into a doublet and slow migrating species in insoluble extracts, which are decreased by treatment with hPOC5 siRNA1. An insoluble polypeptide of ~45 kD that is not affected by RNAi, likely resulting from a cross-reaction, is indicated by an asterisk. Ins, insoluble; Lys, lysate. (e) Anti-hPOC5 but not control antibody immunoprecipitated endogenous hCen2/3 from HeLa cell lysates (left). Similarly, endogenous hPOC5 was immunoprecipitated by anti-hCen2 and anti-hCen3 (right). SN, IP supernatant; IP, immunoprecipitated material. (b–e) Molecular mass is indicated in kilodaltons.

apparent molecular weights. When treated with λ-phosphatase, the mitotic isoforms were shifted back to an apparent molecular weight similar to the interphase forms. Thus, soluble hPOC5 is phosphorylated during mitosis, and centrosome-associated hPOC5 appears to undergo additional phosphorylation events.

Finally, immunogold labeling experiments were performed to study the distribution of hPOC5 at the ultrastructural level (Fig. 3 f). Thin sections of HeLa cells were labeled with anti-hPOC5 (10-nm gold particles) and anti-hCen3 antibody (5-nm gold particles) using a postembedding technique. Appropriate sections of centrosomes show that the 10-nm gold is found predominantly in the distal part of centrioles, colocalizing to a large extent with the 5-nm gold label representing hCen3.

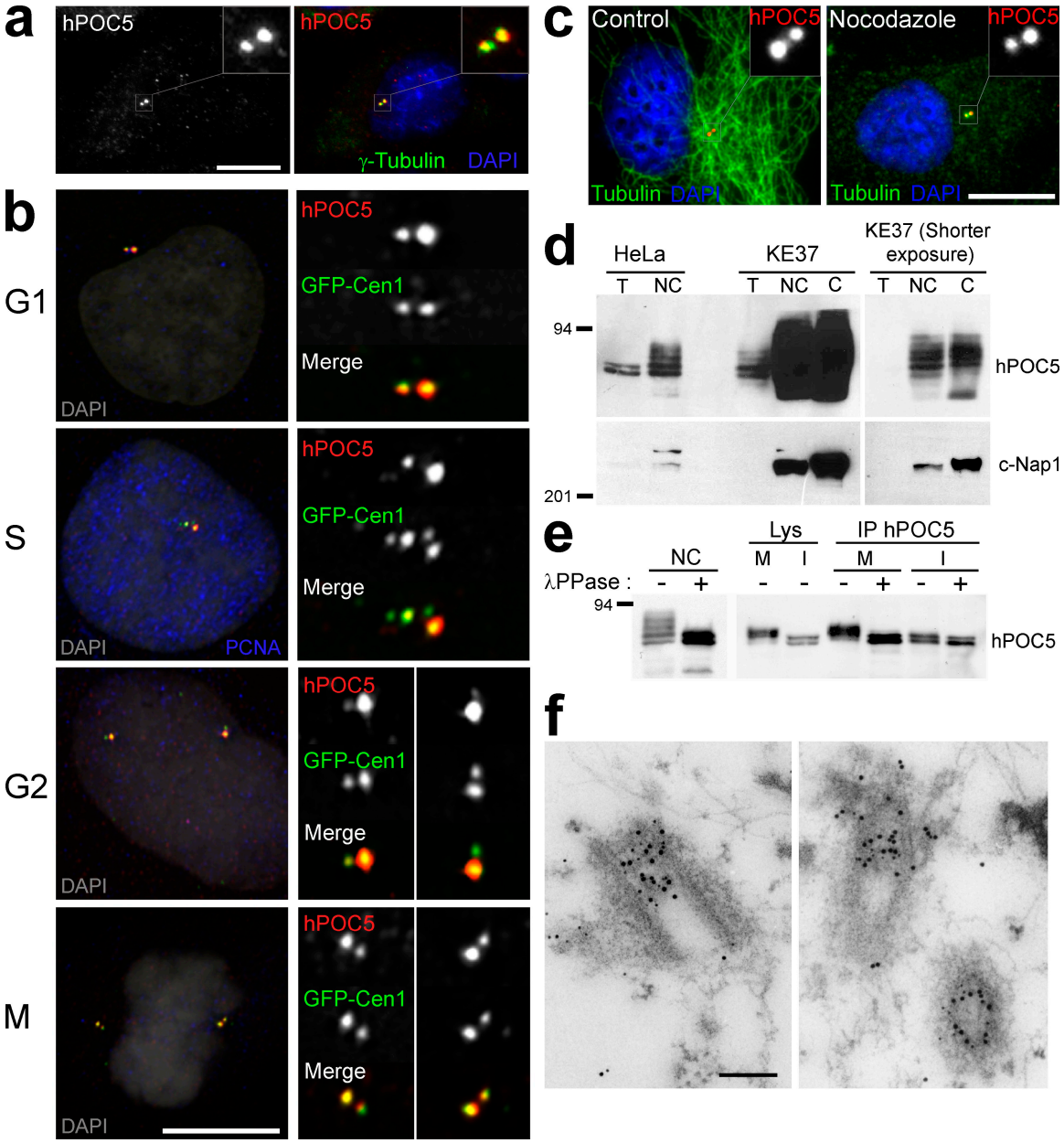

Figure 3. **hPOC5 is a centriolar phosphoprotein.** (a) HeLa cell stained with affinity-purified anti-hPOC5 antibody (shown in red) and anti–γ-tubulin antibody (shown in green). DAPI is shown in blue. (b) Localization of hPOC5 during the cell cycle. RPE1 cells expressing the GFP-Cen1 construct were labeled with affinity-purified anti-hPOC5 and anti-PCNA antibody. S cells exhibit a nuclear PCNA staining; among PCNA-negative cells, GFP-Cen1 allows us to distinguish G1 cells that have a single centrosome from G2 cells that have duplicated centrosomes. hPOC5 is shown in red, GFP-Cen1 is shown in green, PCNA is shown in blue, and DAPI is shown in gray on merged pseudocolor images. (c) Control or nocodazole-treated HeLa cells labeled with anti-hPOC5 (red) and anti-tubulin (green). DAPI is shown in blue. (d) hPOC5 is highly enriched in centrosome fractions. Centrosome-nucleus (NC) or isolated centrosome (C) fractions prepared from HeLa and KE37 cells or KE37 cells only, respectively, were stained with anti-hPOC5 or anti–C-Nap1 as a marker. T, total protein extract. (e) hPOC5 is a phosphoprotein. (left) Centrosome-nucleus fractions were incubated with λ-phosphatase (+) or buffer alone (−) and stained with anti-hPOC5. (right) hPOC5 immunoprecipitated from mitotic (M) or interphase (I) HeLa cell lysates was incubated with λ-phosphatase (+) or buffer alone (−) and revealed with anti-hPOC5. Lys, lysate; IP, immunoprecipitated material. (d and e) Molecular mass is indicated in kilodaltons. (f) Postembedding immunogold colocalization of hPOC5 (10-nm gold particles) and hCen3 (5-nm gold particles) in HeLa cells. (a and c) Insets show magnifications of the boxed areas. Bars: (a–c) 10 μm; (f) 0.2 μm.

hPOC5 is stably incorporated in mother centrioles

To determine the function of hPOC5, we reduced its cellular protein level using siRNAs. Treatment of HeLa cells with specific siRNAs significantly reduced hPOC5 protein levels as compared with control siRNA (Fig. 4 a). Approximately 90% of control interphase cells had two brightly stained centrioles (Fig. 4, b and d). In contrast, in hPOC5-depleted HeLa cells, up to 90% of the cells had only one centriole labeled by anti-hPOC5 antibody (Fig. 4 d).

This phenotype could be caused by the inhibition of centriole duplication leading to a reduced number of centrioles. Alternatively, centriolar structures may assemble without incorporating hPOC5. Colabeling with other centriolar markers such as centrin (Fig. 4 b) or polyglutamylated tubulin (Fig. 4 c) revealed that

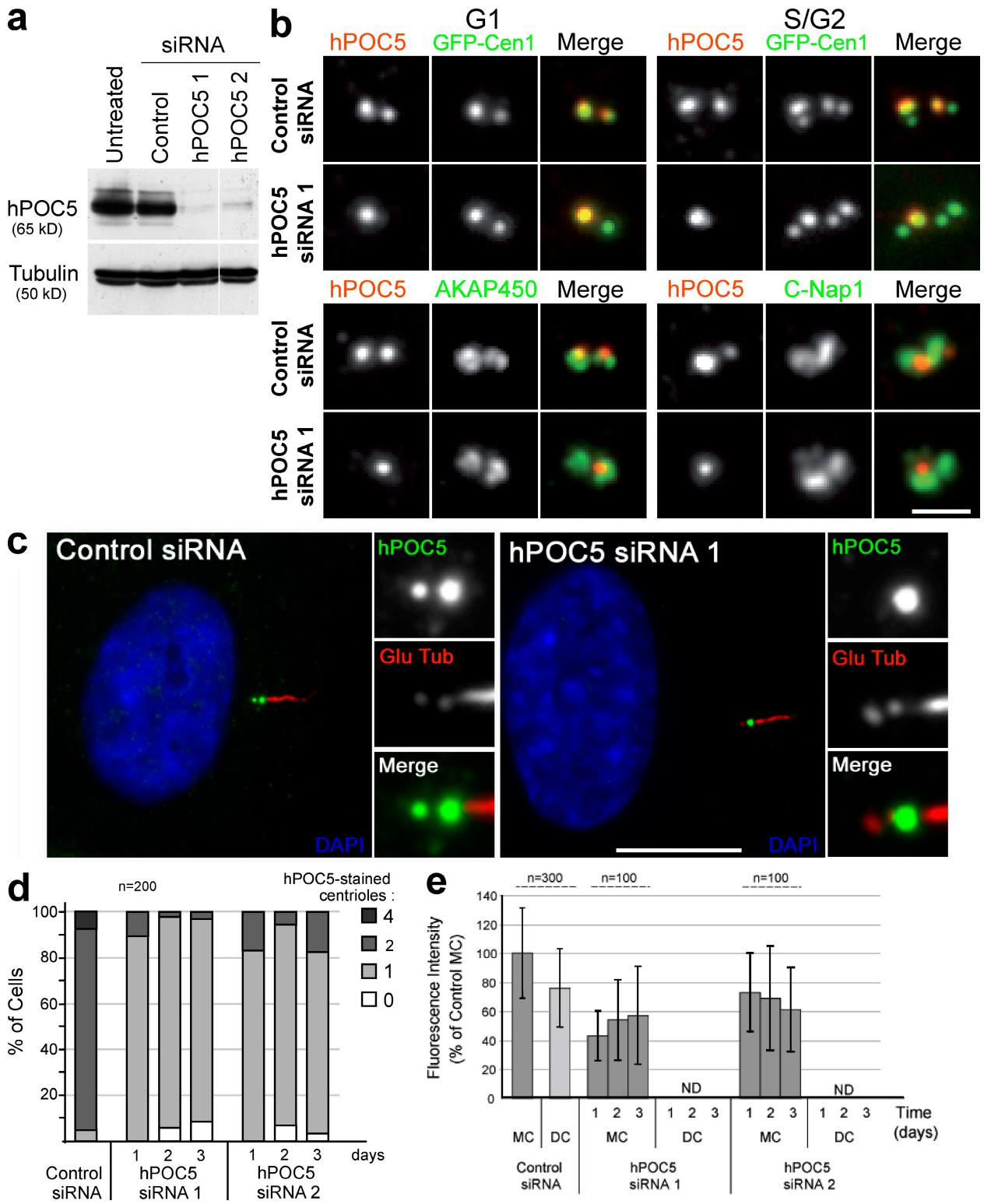

Figure 4. **hPOC5 is stably incorporated into mother centrioles.** (a) hPOC5 levels in HeLa cells treated for 48 h with two different hPOC5 siRNAs or control siRNA. Anti-tubulin was used as a loading control. (b, top) G1 (left) or S/G2 (right) GFP-Cen1–expressing cells treated with control or hPOC5 siRNA 1 for 48 h and stained with anti-hPOC5 (red). (bottom) siRNA-treated HeLa cells labeled with anti-hPOC5 (red) and CTR453 antibody recognizing centrosome-associated AKAP450 or anti–C-Nap1 (green). (c) RPE1 cells treated with control or hPOC5 siRNA 1 and stained with anti-hPOC5 (green) and anti–polyglutamylated tubulin antibody GT335 (Glu Tub; red). DAPI is shown in blue. Insets show magnifications of the centrosome area. (d) Quantification of the number of centrioles labeled by anti-hPOC5 in control and hPOC5 siRNA–treated cells over time. Values are from a single experiment representative of four experiments. (e) Quantification of hPOC5 levels in GFP-Cen1–expressing cells treated with hPOC5 siRNAs for 1–3 d. The values are shown as percentages of the mean fluorescence intensity of the mother centriole in control cells. In hPOC5-depleted cells, hPOC5 fluorescence intensity associated with daughter centrioles labeled by GFP-Cen1 was indistinguishable from the background levels and could not be quantified using the same method (ND). Results were obtained from three different experiments. Error bars represent SD. (d and e) n = total number of cells counted. Bars: (b) 1 µm; (c) 10 µm.

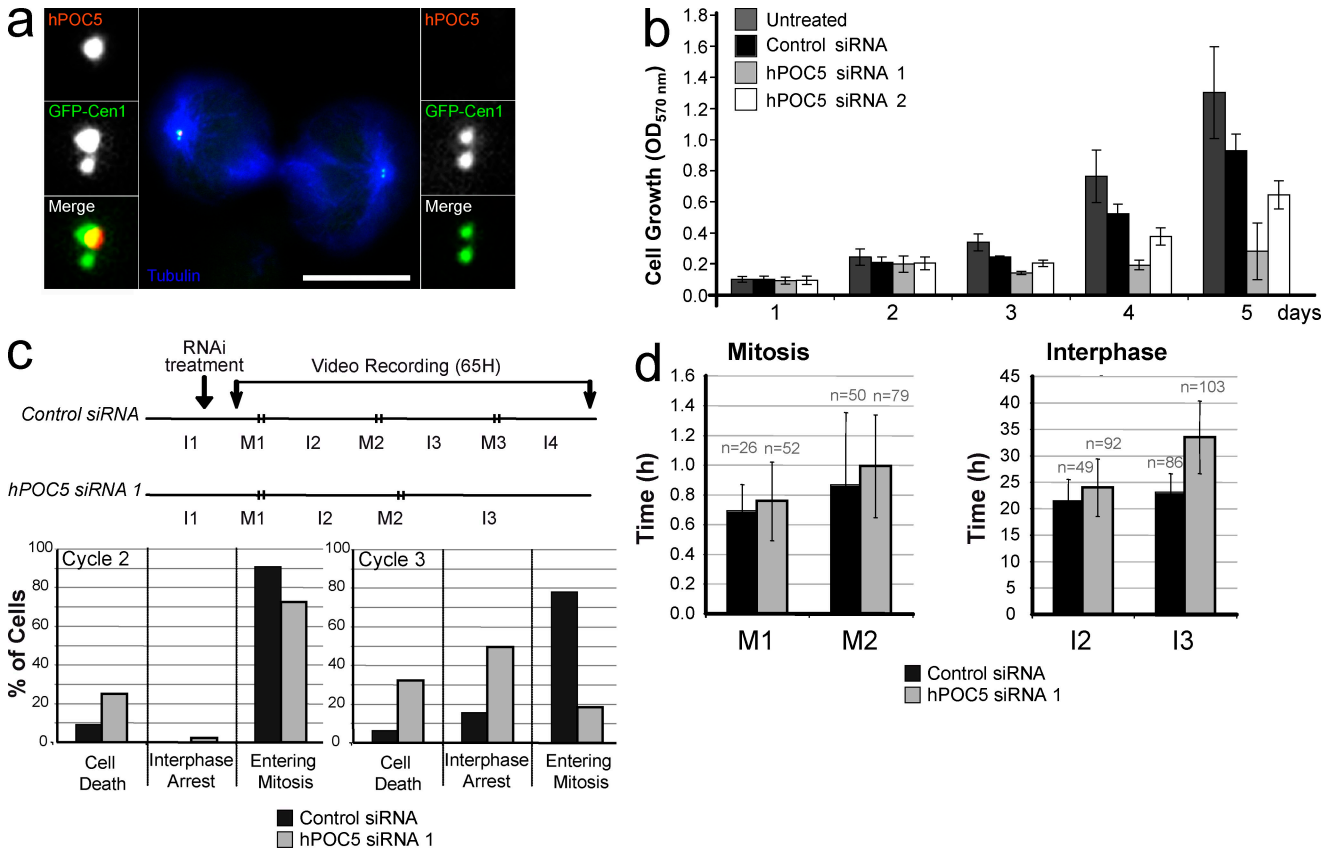

Figure 5. **hPOC5 is an essential protein.** (a) Dividing GFP-Cen1–expressing HeLa cells after 48-h treatment with hPOC5 siRNA 1 and stained with anti-hPOC5 (red) and anti-tubulin (blue). Insets show magnifications of each spindle pole area. (b) Cell growth is affected by hPOC5 depletion. HeLa cells were siRNA treated twice at t = 0 and 2 d later and fixed at designated time points, and cell growth was determined after violet crystal staining (OD_{570}). Results were obtained from three independent measurements in three independent experiments. Mean values ± SD are shown. (c) Fate of HeLa cells treated with hPOC5 siRNA 1 observed by time-lapse imaging. (top) Experimental protocol. Asynchronous HeLa cells were treated with hPOC5 siRNA 1 or control siRNA and video recorded for 65 h starting 6 h after the beginning of siRNA treatment. I, interphase; M, mitosis. (bottom) Percentages of interphase cells that either died, arrested in interphase until the end of the recording, or entered mitosis during interphase 2 (left) or 3 (right). (d) hPOC5-depleted cells exhibit a delay in interphase. Duration of mitosis and interphase of HeLa cells treated with hPOC5 siRNA 1 or control siRNA. Results in c and d were obtained by analysis of time-lapse images of individual cells from two independent experiments. n = total number of cells counted. Error bars represent SD. Bar, 10 μm.

centriolar structures depleted of hPOC5 were present. The amounts of pericentriolar proteins AKAP450 and C-Nap1 associated to centrioles appeared similar in hPOC5-depleted cells and in control cells (Fig. 4 b, bottom). In hPOC5-depleted GFP-Cen1–expressing cells, anti-hPOC5 staining was associated with one of two (in G1 and early S cells) or one of four (in S/G2/M cells) GFP-stained centrioles (Fig. 4 b, top). Similar results were obtained for cells with endogenous centrin proteins stained with 20H5 monoclonal antibody (Fig. S1; Salisbury et al., 2002). The remaining hPOC5 staining was associated with the more brightly GFP-Cen1–stained centriole (Fig. 4 b), which has been shown to be the mother centriole (Piel et al., 2000). This result was confirmed using ciliated RPE1 cells. In siRNA-treated RPE1 cells, the remaining hPOC5 signal was always associated with the mother centriole that nucleates the cilium (Fig. 4 c). Thus, centrosome duplication occurred in hPOC5 siRNA–treated cells, but the nonmature centrioles assembled during the last two cell cycles were devoid of hPOC5.

The mean hPOC5 fluorescence intensity associated with the mother centriole in hPOC5 siRNA–treated cells was 40 ± 20% of that of control cells (Fig. 4 e). This intensity likely represents the amount of hPOC5 that is stably incorporated into centrioles. In contrast, hPOC5 was not detected at the younger, immature centrioles either because it was not incorporated in centrioles that formed after the siRNA treatment or because it was not stably associated to immature centrioles.

hPOC5 is an essential protein

We found that upon hPOC5 siRNA treatment, centrioles lacking hPOC5 but containing other centriolar markers were assembled. If siRNA-treated cells were progressing through the cell cycle, we would expect to observe an accumulation of cells containing no hPOC5-stained centriole because of the dilution over successive cell divisions of the mature centrioles formed before hPOC5 depletion. However, this was not the case, as most of the cells retained one hPOC5-containing mother centriole even at 72 h after siRNA treatment (Fig. 4 d). We could observe mitotic cells in which only the mother centriole was hPOC5 stained (Fig. 5 a), but we could not trace such cells past telophase (Fig. 5 a). In particular, we did not find daughter cells connected by a midbody with hPOC5-free centrosomes. This suggests that these cells are not viable. Therefore, we analyzed the growth of cells

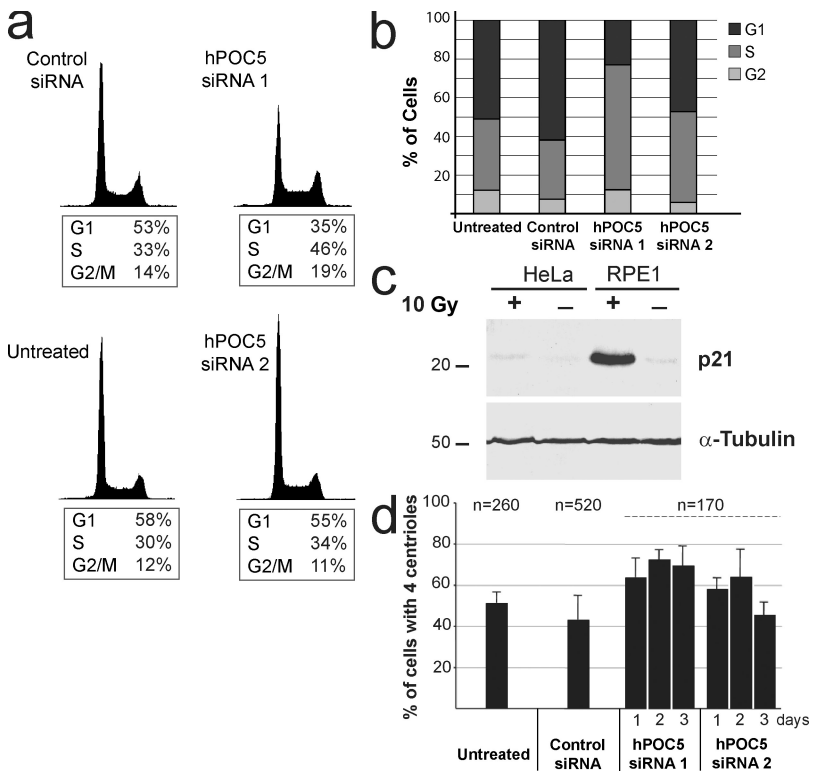

Figure 6. **hPOC5-depleted cells arrest in S phase.** (a) HeLa cells were treated with hPOC5 siRNAs for 72 h and analyzed by flow cytometry. Results are from a single experiment representative of three experiments. (b) Cell cycle analysis of hPOC5- or control siRNA–treated GFP-Cen1 HeLa cells after BrdU incorporation and cyclin B1 staining. Results were obtained from two independent experiments. (c) HeLa and RPE1 cells were irradiated with 10 Gy of γ irradiation and subjected to Western blot analysis. α-Tubulin was used as a loading control. Molecular mass is indicated in kilodaltons. (d) siRNA-depleted cells accumulate in S phase with duplicated centrosomes. RNAi was performed in GFP-Cen1–expressing cells, and the number of GFP-stained centrioles per cell was counted. Results were obtained from three independent experiments. n = total number of cells counted. Error bars represent SD.

depleted of hPOC5. As shown in Fig. 5 b, cells treated with hPOC5 siRNA 1, which induces the strongest hPOC5 depletion (Fig. 4, a and e), exhibited a severe growth defect. siRNA 2 had a milder effect but, nevertheless, induced a significant decrease in cell number. To determine how cell growth was affected, we used video recording of nonsynchronized HeLa cells treated with hPOC5 siRNA 1 (Fig. 5, c and d) starting ∼6 h after the beginning of the siRNA treatment. The fate of cells entering mitosis 0–8 h after the beginning of recording was analyzed over a time period of 65 h. As expected, ∼80% of control cells went through three rounds of mitosis (Fig. 5 c). The mean durations of interphase and mitosis (Fig. 5 d) were very similar for the successive cell cycles (mean of 22.3 ± 3.9 h for interphase and 53 ± 26 min for mitosis). In contrast, only ∼20% of cells entered a third mitosis in hPOC5 siRNA 1–treated cells. Although the duration of interphase 2 (23.9 ± 5.4 h) and mitosis 2 (53 ± 20 min) were similar to control cells, most cells seemed to be delayed during interphase 3, as they had not entered a third mitosis at the end of the time lapse (33.4 ± 6.7 h). In addition, we observed a significant increase in the rate of cell death in hPOC5-depleted cells during both cell cycles 2 and 3 (25% and 32% of the interphase cells, respectively) as compared with control cells (9% and 6% of the cells, respectively). Thus, HeLa cells depleted of hPOC5 have a growth defect, which results from interphase delay and cell death.

hPOC5-depleted cells arrest during S phase in a p53- and p21-independent manner

To determine whether cells were arrested at a particular stage of interphase, we analyzed hPOC5-depleted cells by flow cytometry (Fig. 6 a). In HeLa cells treated with hPOC5 siRNA 1 for 72 h, we observed a significant increase in the proportion of S-phase cells (46% compared with ∼30% in controls). We confirmed these results by analyzing BrdU incorporation, as revealed by immunostaining: hPOC5-depleted cells showed a higher proportion of BrdU-positive cells when compared with control cells (65% vs. 30–35%; Fig. 6 b). A defect in S-phase progression was not observed after simultaneous depletion of hCen2 and hCen3 or after depletion of hSfi1, which is the human homologue of yeast Sfi1p, suggesting that progression through S phase is specifically affected by hPOC5 depletion (Fig. S3).

It has been shown that nontransformed cells like RPE1 cells arrest at the G1/S transition of the cell cycle after the depletion of a variety of centrosome components and that this arrest is p53 and p21 dependent (Srsen et al., 2006; Mikule et al., 2007). Accordingly, we observed that a fraction of RPE1 cells treated with hPOC5 siRNAs arrested in G1 phase (Fig. S2). In HeLa cells, p53 is inactivated by the expression of human papillomavirus proteins E6 and E7, and this G1 arrest is not observed (Srsen et al., 2006). We confirmed that p53 is fully inactive in our HeLa cell line by analyzing the induction of p21 in response to irradiation. DNA damage induced by irradiation is known to induce up-regulation of p53, which, in turn, induces p21 up-regulation. After γ irradiation with 10 Gy, RPE1 cells exhibited a robust p21 up-regulation (Fig. 6 c). In contrast, p21 was not up-regulated in HeLa cells, confirming that p53 is inactive in this cell line. Thus, the mechanism by which hPOC5 inactivation induces a delay in S-phase progression in HeLa cells is distinct from the G1/S-phase arrest induced by centrosome disruption in RPE1 cells.

hPOC5-depleted cells exhibited an extended S phase, during which the assembly of procentrioles normally occurs. Accordingly, the proportion of cells with two pairs of dots labeled with GFP-Cen1 was increased in hPOC5 siRNA–treated HeLa

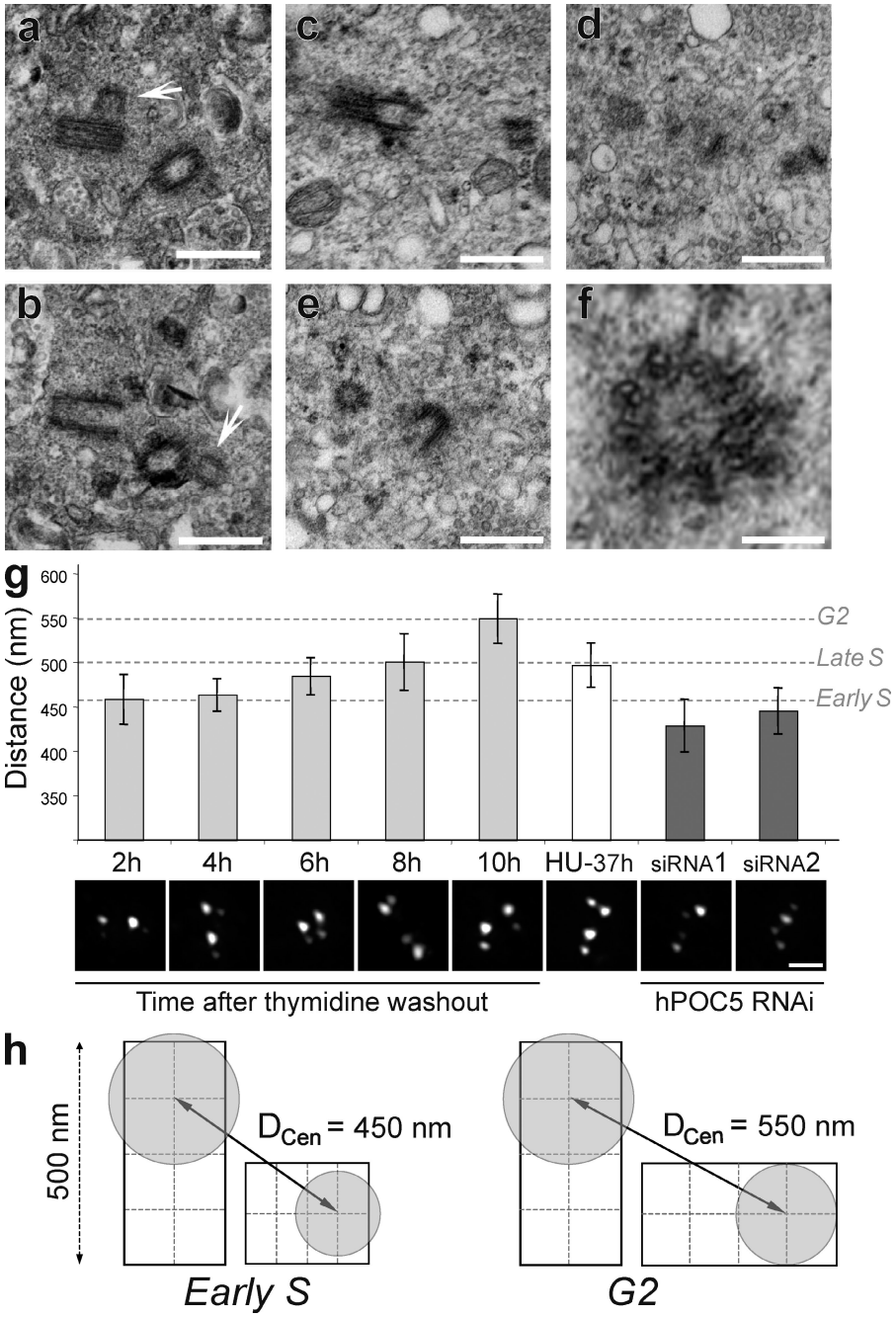

Figure 7. **hPOC5-depleted HeLa cells accumulate with short procentrioles.** (a and b) HeLa cells treated with hPOC5 siRNA 1 for 48 or 72 h were glutaraldehyde fixed and randomly selected for serial-thin sectioning. Panels a and b show two consecutive sections of the same centrosome. Arrows show the procentrioles. (c–e) HeLa cells were treated with siRNA 1 for 48 h, and round-shaped cells were collected by mitotic shake-off and glutaraldehyde fixed. Panels c, d, and e show three consecutive sections of the same centrosome. Panel f shows a magnification of the procentriole seen in the transverse section in e. (g) Elongation of the procentriole was estimated by measuring the distance between the center of mass of the two dots of GFP-Cen1 staining within each pair of orthogonally arranged centrioles (D_{Cen}) in GFP-Cen1–expressing HeLa cells with duplicated centrosomes. The graph shows the mean value of the highest 20% of values obtained from series of 100 measurements ± SD. The highest values are obtained when D_{Cen} is parallel to the plan of imaging and, thus, represent a better approximation of the real distance. D_{Cen} was measured in control cells synchronized by a double thymidine block at the indicated time points after thymidine washout (2–10 h) as well as in synchronized control cells arrested in S phase by HU treatment for 37 h (HU-37 h). These values were compared with D_{Cen} measured in cells treated by hPOC5 siRNAs 1 and 2 that exhibited duplicated centrosomes. Micrographs show the GFP-Cen1 staining in a representative cell for each condition. (h) Schematic representation of D_{Cen} measured in diplosomes from early S- or G2-phase cells. The center of mass of the GFP staining (gray circles) is assumed to be centered on the distal end of each centriole. Bars: (a–e) 0.5 μm; (f) 0.1 μm.

cells compared with control cells (Fig. 6 d). After the treatment with hPOC5 siRNA 1, the proportion of cells with duplicated centrosomes reached ∼70% after 48–72 h, as compared with ∼45% for controls. Thus, hPOC5 depletion induces an accumulation of cells in S phase where procentriole assembly has been apparently properly initiated.

Procentriole elongation is blocked in hPOC5-depleted cells

To determine whether hPOC5-depleted cells were arrested at a specific stage of procentriole assembly, we used EM of serial-sectioned HeLa cells treated with hPOC5 siRNA 1. As siRNA treatment affects a large proportion of cells (∼90%), the cells subjected to serial sectioning were selected randomly. 14 interphase cells corresponding to two pairs of postmitotic cells connected by a cytoplasmic bridge and 10 individual cells were analyzed. Each of the four cells forming the two pairs had one centrosome containing two full-length centrioles. Among the 10 individual cells, 9 had duplicated centrosomes, each containing a full-length centriole and an orthogonally arranged procentriole (Fig. 7, a and b). In these cells, the length of the procentrioles was 39% of the length of mature centrioles (180 ± 50 nm for procentrioles vs. 458 ± 77 nm for mature centrioles). In addition, the diameter of these procentrioles appeared smaller in longitudinal sections (Fig. 7, a and b). Accordingly, transverse sections revealed that procentrioles were formed by doublet microtubules instead of triplets (Fig. 7, e and f). Procentrioles of similar length and diameter have been shown to correspond to an early step of centriole duplication, taking place

during early S phase in human cell lines (Robbins et al., 1968; Loncarek et al., 2008). To determine more precisely at which step of the centrosome duplication cycle procentrioles of similar length are normally observed, we used centrin staining as a marker for procentriole elongation. It has been shown that the distance separating the two dots of centrin staining associated to a pair of orthogonally oriented centrioles increases during progression into S and G2 phases, reflecting the elongation of the procentriole (Piel et al., 2000; Loncarek et al., 2008). To further establish that the distance between centrin dots (D_{Cen}; Fig. 7 h) can provide a quantitative estimation of procentriole elongation, we measured D_{Cen} at various steps of centrosome duplication (Fig. 7 g). GFP-Cen1–expressing HeLa cells were synchronized at the G1/S boundary by a double thymidine block and fixed every 2 h after thymidine washout. The experiment was carried on until the onset of the mitotic wave (10 h after washout). At that time point, measurements were obtained from cells that had not yet rounded up for mitosis, which were likely to be in the G2 phase of the cell cycle. We observed a gradual increase in the mean value of D_{Cen} as cells progressed through S and G2 phases, confirming that centrin staining is a reliable marker for procentriole elongation (Fig. 7 g). We then measured D_{Cen} in cells depleted from hPOC5 over 72 h and found that for both hPOC5 siRNAs, the mean value of D_{Cen} was less than in synchronized cells 2 h after thymidine washout. This result strongly supports the fact that procentrioles in hPOC5-depleted cells are similar in length to procentrioles observed during early steps of centrosome duplication, which is in agreement with our EM observations (Fig. 7 g). It has been shown that procentriole elongation only partially takes place in cells arrested in S phase for prolonged periods (Rattner and Phillips, 1973; Loncarek et al., 2008). However, comparing EM data obtained by Loncarek et al. (2008) using the same cell line with this study supports the fact that procentrioles extend further in hydroxyurea (HU)-arrested cells than in hPOC5-depleted cells. To confirm this observation, we measured D_{Cen} in HeLa cells synchronized by mitotic shake-off and cultured in the presence of HU for 37 h, which is an amount of time similar to that used previously (40 h; Loncarek et al., 2008) and similar to the interphase arrest in hPOC5-depleted cells (33.4 h; Fig. 5 d, I3). In HU-arrested cells, the mean value of D_{Cen} was similar to what we measured in late S-phase cells (8 h after thymidine washout) and, thus, was significantly higher ($P < 2 \times 10^{-06}$) than in hPOC5-depleted cells. Interestingly, D_{Cen} in HU-treated cells did not reach the G2-phase value (10 h after thymidine washout) despite the prolonged S-phase arrest, suggesting that the transition into G2 phase is required for further elongation of the procentrioles (Fig. 7 g).

Finally, we wanted to look at the ultrastructure of centrioles in hPOC5-depleted cells that were able to enter mitosis. To this aim, we collected cells by mitotic shake-off 48 h after incubation with hPOC5 siRNA 1. However, we found that a vast majority of these cells were not in mitosis despite their round shape. Six of these cells were subjected to serial sectioning and EM analysis. Five of them had duplicated centrioles with short, cartwheel-containing procentrioles, confirming our observations on spread interphase cells (Fig. 7, c–f). In addition, some procentrioles were disengaged from the parental centriole wall in three of these cells (Fig. S4).

To summarize, hPOC5-depleted cells are able to initiate the assembly of procentrioles, but these procentrioles fail to elongate. Furthermore, this defect in procentriole elongation is clearly distinct from what is observed in cells arrested in S phase by HU and, thus, appears to be a direct consequence of hPOC5 depletion rather than a secondary effect of S-phase arrest.

Discussion

hPOC5 defines a new family of centrin-binding proteins that share a tandem of Sfi1p repeats that can bind both hCen2 and hCen3 in vitro. The noncentrosomal pool of hPOC5 physiologically interacts with hCen2 and hCen3, and the centrosome-associated hPOC5 colocalizes with both centrin proteins in the distal lumen of the centriole, in which a conspicuous and poorly characterized structure is present (Paintrand et al., 1992). Unlike centrin, hPOC5 is recruited in centrioles late in the duplication process, namely during G2/M. In the absence of hPOC5, HeLa cells accumulate in S phase. In these cells, centriole duplication has been initiated, but the procentrioles subsequently fail to elongate. Therefore, hPOC5 is essential for the assembly of full-length centrioles and for cell proliferation. Our results further suggest that the assembly of proximal and distal parts of centrioles is controlled separately and that hPOC5 is required for the latter part of this process.

hPOC5 is a centriolar centrin-binding protein

Centrin has been shown to be one of the very first proteins recruited at procentriole assembly sites (Middendorp et al., 1997; Klink and Wolniak, 2001; Koblenz et al., 2003; Stemm-Wolf et al., 2005). In mammalian cells, centrin is recruited there during early S phase, before the assembly of procentriole microtubules (Middendorp et al., 1997). In contrast, hPOC5 was not detected in the procentrioles before G2. Thus, it is likely that other centrin-interacting proteins are involved in the initial steps of procentriole assembly. In addition, centrin proteins appear to have partners within the distal part of elongated centrioles, as hPOC5-depleted centrioles are still positive for centrin staining, although to a lesser extent than control centrioles (Figs. 5 a and 7 g). Candidate centriolar centrin-interacting proteins include the vertebrate homologue of Sfi1p and CP110 protein, although a direct interaction has not been demonstrated for the latter (Kilmartin, 2003; Tsang et al., 2006).

After hPOC5 is first detected at the distal end of procentrioles in G2/M, it keeps accumulating during the next cell cycle together with hCen2/3 proteins. We show that the hPOC5 soluble pool is phosphorylated during mitosis and that the centriole-associated hPOC5 fraction is hyperphosphorylated, suggesting a possible phosphorylation-dependent recruitment of hPOC5 to the centriole. The progressive recruitment of hPOC5 in centrioles suggests that it may play a role in centriole maturation.

hPOC5 is required for cell cycle progression

We found that in the absence of hPOC5, HeLa cells accumulate in S phase, whereas RPE1 cells arrest in G1 phase. Previous studies have shown that, in nontransformed cell lines like RPE1, affecting centrosome integrity by depleting or mislocalizing a

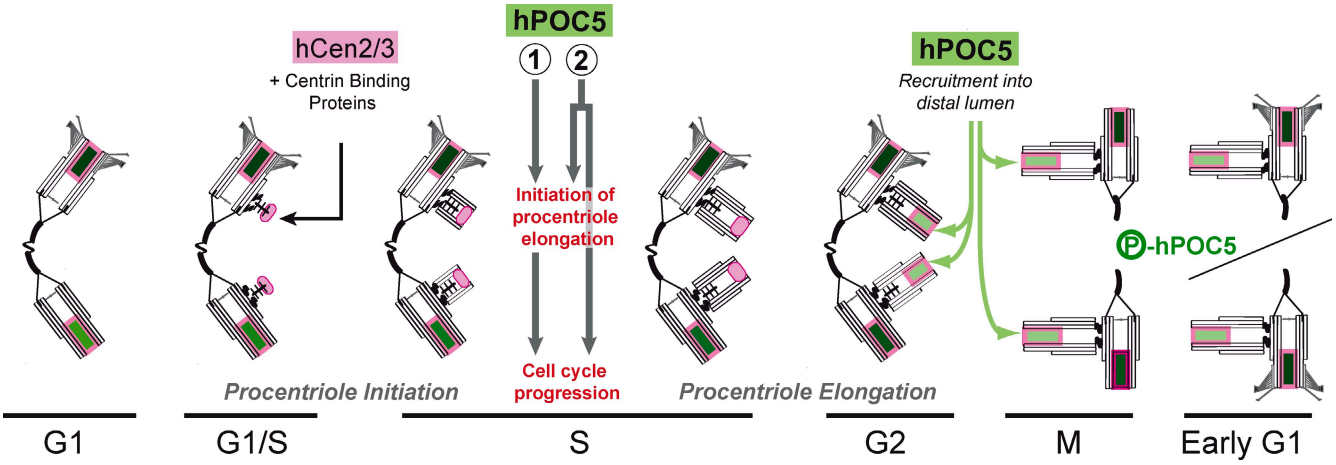

Figure 8. **Model for the role of hPOC5 in centriole assembly.** In control cells, the duplication starts during late G1 or early S phase by the assembly of a precursor structure containing a cartwheel that contains centrin proteins (shaded in pink) but not hPOC5. Centrin proteins are likely to interact at this step with another unidentified centrin-binding protein. During early S phase, microtubule singlets then doublets are assembled around the cartwheel. During mid or late S phase, either (1) hPOC5 is required to initiate procentriole elongation and this, in turn, allows cell cycle progression, or (2) hPOC5 triggers procentriole elongation and performs an additional function required for progression through S phase independently. During G2 phase, hPOC5 (shaded in green) starts to accumulate in the distal lumen of procentrioles, concomitantly to its phosphorylation, and keeps accumulating during the subsequent cell cycle together with centrin.

wide range of centrosomal components leads to a cell cycle arrest at the G1/S transition (Srsen et al., 2006; Mikule et al., 2007). This arrest occurs before the initiation of centrosome duplication and of DNA replication and is p38, p53, and p21 dependent (Srsen et al., 2006; Mikule et al., 2007). In addition to centrosome disruption, exogenous stress can also arrest RPE1 cells in G1, suggesting that this arrest results from a broader range stress response (Uetake et al., 2007). The similarities between our results and the aforementioned studies suggest that hPOC5 depletion induces the same stress response in RPE1 cells. In contrast, p53-defective cell lines like HeLa cells do not arrest in G1 after centrosome disruption (Srsen et al., 2006). We confirmed that p53 was fully inactive in the HeLa cells used in this study, as revealed by the lack of p21 up-regulation after irradiation. We found that hPOC5-depleted HeLa cells were able to enter S phase, as supported by the fact that both initiation of centrosome duplication and DNA replication were taking place in these cells, but eventually failed to enter mitosis and underwent cell death. Our results point to a specific requirement for hPOC5 during progression through S phase. However, whether the observed defect in cell cycle progression results from hPOC5 centriolar functions or from separate functions is not known at present.

hPOC5 is required for centriole elongation

Our results show that most of hPOC5-depleted cells arrest with duplicated centrosomes, each containing one full-length parental centriole and one short procentriole. EM of serial-sectioned cells revealed that the procentrioles are ~40% as long as full-length centrioles. In addition, the procentrioles retain features normally observed during early initiation of centriole duplication: they are formed of doublet microtubules instead of triplets, and they contain a very well-defined cartwheel structure, which are all features that are typical in procentrioles found during early S phase in mammalian cells (Robbins et al., 1968). We confirmed by fluorescence microscopy using centrin staining as a marker for procentriole elongation that procentrioles in hPOC5-depleted cells are similar in length to these found during early steps of centrosome duplication.

In mammalian cells, initiation of centriole duplication is followed by elongation of the procentrioles during S and G2 phases (Kuriyama and Borisy, 1981; Vorobjev and Chentsov Yu, 1982; Chretien et al., 1997). This process has been proposed to depend on cell cycle progression, as procentrioles in cells arrested in S phase by DNA synthesis inhibitors are only partially elongated (Rattner and Phillips, 1973; Loncarek et al., 2008). Our results confirm these observations and further show that procentrioles in HU-arrested cells can reach the maximal length observed in control S-phase cells but that additional elongation requires transition into G2 phase. Procentrioles assembled in the absence of hPOC5 are clearly shorter and narrower than the procentrioles observed by EM in cycling HeLa cells during late S phase (Robbins et al., 1968) or in the HeLa cells arrested in S phase with HU (Loncarek et al., 2008). This conclusion is also strongly supported by our analysis of centrin staining. Together, our results suggest that initiation of centriole duplication occurs in the absence of hPOC5 but that subsequent elongation is inhibited. The observed defect is markedly distinct from the partial elongation in drug-induced S-phase arrest, which suggests that hPOC5 is directly required for centriole elongation.

It is intriguing that hPOC5 depletion affects procentriole assembly during early S phase, as hPOC5 is first detected at the procentrioles during G2 phase in control cells (Fig. 3 b). Also, hPOC5 siRNA–treated cells contain an apparently full-length daughter centriole that is devoid of hPOC5 during the cell cycle preceding the S-phase arrest. Thus, hPOC5 may be required to regulate centriole elongation before its incorporation within procentrioles (Fig. 8). This could imply the existence of an intra–S phase mechanism regulating centriole duplication. Alternatively, hPOC5 could be recruited within procentrioles during

S phase in amounts lower than the detection limit in our experimental conditions.

In conclusion, our data show that hPOC5 is a centrin-binding protein essential for centriole elongation and cell cycle progression. Whether the S-phase delay observed in hPOC5-depleted cells results from inhibition of centriole elongation or from another hPOC5-dependent function is an important question that will deserve further work. Our data also support the idea that daughter centrioles are assembled in two main steps coupled to cell cycle progression. The first step corresponds to the assembly of a procentriole organized around a cartwheel structure. The second step, for which hPOC5 is required, corresponds to the assembly of the distal portion of the centriole. This assembly scheme may be related to what occurs in the green algae *C. reinhardtii*. In this species, the two probasal bodies remain of the length of the cartwheel structure for most of interphase, elongating only during G2 phase (Dutcher, 2003; Piasecki et al., 2008). Although occurring in a different timing in human cells, the mechanisms that control the initiation of elongation may be evolutionarily conserved. Interestingly, the genomes of *Drosophila* and *C. elegans*, which are two species that assemble modified short centrioles (Callaini et al., 1997; Pelletier et al., 2006), do not contain POC5 homologues.

Materials and methods

Cell culture

HeLa and RPE1 cells (Clontech Laboratories, Inc.) were cultured in DME or DME/F-12 (Invitrogen), respectively, supplemented with 10% fetal calf serum (Biowest), 100 U/ml penicillin, and 100 µg/ml streptomycin (Invitrogen). HeLa cells expressing GFP-hCen1 have been described previously (Piel et al., 2000). RPE1 cells expressing the same construct were obtained according to the same protocol. For D_{Cen} measurements, GFP-Cen1–expressing HeLa cells were either synchronized by a double thymidine block (18-h block, 10-h release, and 14-h block) using 2 mM thymidine or collected by mitotic shake-off and were replated in the presence of 2 mM HU for 37 h.

Cell irradiation

Cells grown to semiconfluency were irradiated (10 Gy) in PBS at RT using a ^{137}Cs source. After 7 h at 37°C in normal medium, cells were scrapped in PBS and sedimented at low speed, and the pellet was solubilized in boiling sample buffer for SDS-PAGE analysis.

Yeast two-hybrid analysis

A cDNA encoding full-length hCen2 was cloned into the pB29 bait plasmid derived from pFBL23 (Beranger et al., 1997). A C-terminal domain of hCen2 (aa 93–173) was inserted into the pB27 bait plasmid derived from the original pBTM116 (Vojtek and Hollenberg, 1995). Random-primed cDNA libraries from human placenta and the PAZ-6 cell line (preadipocyte) poly(A)$^+$ RNA were constructed into the pP6 plasmid derived from the original pGADGH (Bartel et al., 1993). The libraries were transformed into the Y187 yeast strain, and 10^7 independent yeast colonies were collected, pooled, and stored at −80°C as equivalent aliquot fractions of the same library. The screens were performed to ensure a minimum of 5×10^7 interactions tested using a mating protocol previously described (Fromont-Racine et al., 1997). Prey fragments of the positive clones were amplified by PCR and sequenced at their 5′ and 3′ junctions on a sequencer (PE3700; Applied Biosystems). The resulting sequences were used to identify the corresponding gene in the GenBank database (National Center for Biotechnology Information) using a fully automated procedure.

hPOC5 cloning and bioinformatics analyses

Reverse transcription was performed on HeLa cell total RNA extracts using the hPOC5-specific primer, 5′-AACCAAAAGACTTCTAACCCTT-3′. hPOC5 single-strand cDNA was amplified by two successive PCR reactions using reverse transcription primer and 5′-TGACACTGCAGCTGCGAC-3′ for the first reaction and 5′-GGAATTCATGTCATCAGATGAG-3′ and 5′-GGGTTAGTCAACCACTTTTATG-3′ for the second reaction. The 1,728-bp cDNA is identical to the N terminus of BC010695 (bp 111–194) and to NM_152408 (bp 51–1694) for the rest of the sequence.

hPOC5 homologues were identified by BLAST (Basic Local Alignment Search Tool) analysis using either full-length hPOC5 or the 21-aa signature sequence (aa 349–369). hPOC5 and homologues were analyzed for coiled-coil regions using MacStripe2.0b1 software (http://www.york.ac.uk/depts/biol/units/coils/mstr2.html). Sequence alignment was performed using ClustalW (http://www.ch.embnet.org/) and drawn using Boxshade at http://www.ch.embnet.org. The phylogenetic tree was constructed with the neighbor-joining method using ClustalW and drawn using Phylodendron at http://www.es.embnet.org/.

GST pull-downs

For coexpression, hPOC5 fragments F1 (aa 1–170), F2 (aa 101–435), and F3 (aa 371–575) were fused with GST in pGEX4-T1. hCen2 and hCen3 were cloned in pET29 (EMD) and cotransfected with F1–3 GST fusions in Rosetta (DE3) *E. coli* host strain (EMD). Bacteria were induced for 4 h at 37°C. Protein extracts (in 50 mM Tris, pH 8, 150 mM NaCl, 1% NP-40, 0.5% deoxycholate, and 10 mM EGTA supplemented with protease inhibitors) were incubated with glutathione–Sepharose 4 Fast Flow (GE Healthcare), and beads were boiled in SDS sample buffer.

CBR_1 (aa 117–197) and CBR_{2+3} (aa 222–304) as well as hCen2/3 and human CaM 2 (available from GenBank/EMBL/DDBJ under accession no. NM_001743) were cloned in pGST-Parallel1 (Sheffield et al., 1999). The GST fusions were produced as described for the F1–3 GST fusions and bound to glutathione beads. hCen2/3 or CaM were digested by tobacco etch virus protease to remove GST and incubated at a concentration of 5 µM with GST-CBR beads. Beads and supernatants were boiled in SDS sample buffer, and equivalent amounts were loaded on a gel.

Antibodies

Full-length hPOC5 was cloned in pET15b vector (EMD) and expressed in *E. coli*. His-hPOC5 was purified under denaturing conditions using Ni-NTA resin (QIAGEN) and dialyzed before rabbit immunization (Agro-Bio). Antibodies were purified over a GST-F1 column and a GST-F3 column and eluted at a low pH. Anti-hCen2 and anti-hCen3 antisera (Laoukili et al., 2000) were purified over a GST-hCen2 or a GST-hCen3 column, respectively. Anti-hCen1 crude antiserum, which cross reacts with hCen2 (Laoukili et al., 2000), was used for Western blot analysis. CTR453 is a monoclonal antibody recognizing exon 29 of human AKAP450 (Keryer et al., 2003). GT335, a monoclonal anti-polyglutamylated tubulin, was a gift from B. Eddé (Université de Paris 6, Paris, France; Wolff et al., 1992). Monoclonal anti–C-Nap1 was purchased from BD, monoclonal anti–proliferating cell nuclear antigen (PCNA) was purchased from Dako, and monoclonal anti–γ-tubulin (clone GTU88) was purchased from Sigma-Aldrich. The secondary antibodies used for immunofluorescence microscopy were Alexa Fluor 488–conjugated (Invitrogen) and Cy3/Cy5-conjugated (Jackson ImmunoResearch Laboratories) donkey IgGs.

Cell fractionation and Western blotting

Nucleus/centrosome fractions from HeLa and KE37 cells were prepared as follows: cells were resuspended at 10^7 cells/ml in lysis buffer (10 mM Tris, pH 7.5, 10 mM NaCl, 3 mM $MgCl_2$, 1% NP-40, and 10% sucrose with protease inhibitors) and centrifuged at 100 g. The pellet containing the nuclei was incubated at RT in the same volume of digestion buffer (10 mM K-Pipes, pH 6.8, 50 mM NaCl, 3 mM $MgCl_2$, 1 mM EGTA, 10% sucrose, 0.1 mg/ml DNase I, and 0.1 mg/ml RNase A with protease inhibitors) for 30 min. After addition of $(NH_4)_2SO_4$ and NaCl at final concentrations of 0.25 M and 1 M, respectively, the extracts were centrifuged at 15,000 *g* over a cushion of 60% sucrose in digestion buffer. The nucleus/centrosome fractions were collected at the 10–60% sucrose interface. Isolated centrosome fractions from KE37 were prepared as previously described (Bornens and Moudjou, 1999) and provided by C. Celati (Institute Curie, Paris, France).

For immunoprecipitation assays, affinity-purified anti-hPOC5, -hCen2, and -hCen3 antibodies or monoclonal anti-myc antibody 9E10 was bound to sheep anti–rabbit or anti–mouse IgG Dynabeads (M-280; Invitrogen), respectively. Beads were incubated with HeLa cell extracts prepared in lysis buffer (50 mM Tris, pH 8, 150 mM NaCl, 1% NP-40, 0.5% deoxycholate, and 0.1% SDS supplemented with protease inhibitors) and analyzed by SDS-PAGE.

Protein dephosphorylation was performed as follows: nucleus/centrosome fractions from HeLa cells or immunoprecipitated hPOC5 bound to Dynabeads (see previous paragraph) were incubated with 1,000 U λ-phosphatase (New England Biolabs, Inc.) in λ-phosphatase buffer supplemented with 2 mM $MnCl_2$, 0.15 M NaCl, and protease inhibitors.

Immunofluorescence

All cells were fixed in cold methanol for 3–5 min except HeLa cells expressing GFP-hCen1 used for analysis of centrosome duplication and for D_{Cen} measurements, which were fixed in 4% paraformaldehyde. BrdU incorporation was performed as described previously (Taddei et al., 1999). All samples were mounted in Mowiol medium (Sigma-Aldrich). Cells were imaged using an upright motorized microscope (DMRXA2; Leica) equipped with an oil 100× NA 1.4 Plan-Apochromat objective and a cooled charge-coupled device camera (CoolSNAP HQ; Photometrics) as described previously (Celton-Morizur et al., 2004). For the measurement of hPOC5 staining intensity, the mean intensity of the most intense 20% of the pixels in the centriole area was quantified on maximal intensity projections of z series (0.2-µm interval) using MetaMorph software (MDS Analytical Technologies). For D_{Cen} measurements, cells were imaged using a deconvolution microscope (Deltavision; Applied Precision, LCC) using a cooled charge-coupled device CoolSNAP HQ camera attached to an inverted microscope (IX70; Olympus). Optical sections were acquired using an oil 100× NA 1.4 Plan-Apochromat objective. softWoRx image processing software (Applied Precision, LCC) was used for acquisition, deconvolution of optical sections, and maximal intensity projection of deconvolved z series (0.2-µm interval). The center of mass of the centrin spots was determined manually on z projections observed at high magnification, and D_{Cen} values were measured using ImageJ software (National Institutes of Health).

EM

For immunogold staining, HeLa cells were grown on plastic coverslips (Thermanox; Thermo Fisher Scientific) for 24 h. They were lysed for 60 s with 1% Triton X-100 in PHEM (Pipes, Hepes, EGTA, and $MgCl_2$) followed by a fixation with 2% formaldehyde in PHEM for 20 min. Dehydration, embedding in Lowicryl (Electron Microscopy Sciences), labeling, and staining were performed as described previously (Euteneuer et al., 1998). Double staining with 5-nm and 10-nm protein A–gold was performed as described previously (Slot et al., 1991).

For EM serial sectioning, cells treated with hPOC5 siRNA 1 were fixed for 1 h in 2.5% glutaraldehyde in 0.1 M cacodylate buffer, pH 7.3. Embedding and serial sectioning for EM were performed according to standard procedures (Rieder and Cassels, 1999).

siRNA

Ready to use double-stranded hPOC5 siRNA 1 (target sequence, 5′-CAACAAATTCTAGTCATA-3′), hPOC5 siRNA 2 (target sequence, 5′-TCCAATGATTATGAAGCCAAA-3′), and control siRNA targeting GL2 luciferase (target sequence, 5′-CGTACGCGGAATACTTCGA-3′) were purchased from QIAGEN. siRNA was delivered into cells using HiPerfect reagent (QIAGEN) in OptiMEM medium (Invitrogen). 4–6 h after transfection, OptiMEM was supplemented with 10% fetal calf serum.

Videomicroscopy

Cells grown on 35-mm glass-base dishes (Asahi Techno Glass Corporation) for 24 h were treated by RNAi. Cells were video recorded starting ∼6 h after the beginning of RNAi treatment using a microscope (DMIBRE; Leica) equipped with a 20× objective and a heated and motorized stage. Cells were imaged by phase-contrast microscopy at the frame rate of one image every 5 min using MetaMorph software. Cells were covered with a porous membrane allowing CO_2 buffering and were maintained at 37°C in the presence of 5% CO_2 during the time of the experiment.

Flow cytometry

Cells were subjected to siRNA treatment for 72 h, harvested, and fixed by drop-wise addition of 3 vol of ice-cold 70% ethanol. After treatment with RNase A (Roche) at 10 mg/ml in PBS, cells were resuspended in 1 mg/ml propidium iodide (Sigma-Aldrich) in PBS and subjected to analysis (FACSort; BD) using CellQuest Pro 4.02 (BD) and ModFit 3.0 (Verity Software House) softwares.

Online supplemental material

Fig. S1 shows that endogenous centrin proteins stained by 20H5 antibody and a GFP-Cen1 fusion protein localize in a similar manner at the centrosome of control or hPOC5-depleted HeLa cells. Fig. S2 shows that a fraction of RPE1 cells depleted of hPOC5 arrest in G1. Fig. S3 shows that HeLa cells accumulate in S phase after depletion of hPOC5 but not after depletion of hSfi1 or simultaneous depletion of hCen2 and hCen3. Fig. S4 shows serial sections through an hPOC5-depleted HeLa cell in which one short procentriole is disengaged from the parental centriole. Online supplemental material is available at http://www.jcb.org/cgi/content/full/jcb.200808082/DC1.

We wish to thank J. Loncarek and V. Favaudon for very useful comments, S. Aresta and L. Daviet for two-hybrid screening, C. Celati for centrosome fractions, J. Salisbury for 20H5 antibody, and B. Eddé for GT335 antibody. We thank Z. Maciorowski and C. Guérin for assistance with flow cytometry experiments, J.-B. Sibarita for assistance with fluorescence intensity measurements, M. Théry and T. Julou for help with video recording, and A. Paoletti for critical reading of the manuscript. We acknowledge use of the Wadsworth Center's Electron Microscopy Core facility.

This work was supported by the GenHomme Network Grant (02490-6088) from Hybrigenics and Institut Curie to M. Bornens, an Agence Nationale de la Recherche grant (NT05-4_42485) to M. Bornens, and a Human Frontier Science Program grant (RGP0064/2004) to M. Bornens and A. Khodjakov. J. Azimzadeh was the recipient of a fellowship from Association pour la Recherche sur le Cancer.

Submitted: 5 August 2008
Accepted: 3 March 2009

References

Adams, I.R., and J.V. Kilmartin. 2000. Spindle pole body duplication: a model for centrosome duplication? *Trends Cell Biol.* 10:329–335.

Andersen, J.S., C.J. Wilkinson, T. Mayor, P. Mortensen, E.A. Nigg, and M. Mann. 2003. Proteomic characterization of the human centrosome by protein correlation profiling. *Nature*. 426:570–574.

Araki, M., C. Masutani, M. Takemura, A. Uchida, K. Sugasawa, J. Kondoh, Y. Ohkuma, and F. Hanaoka. 2001. Centrosome protein centrin 2/caltractin 1 is part of the xeroderma pigmentosum group C complex that initiates global genome nucleotide excision repair. *J. Biol. Chem.* 276:18665–18672.

Azimzadeh, J., and M. Bornens. 2004. The centrosome in evolution. *In* Centrosomes in Development and Disease. E.A. Nigg, editor. Wiley-VCH, Weinheim, Germany. 93–122.

Baroin, A., R. Perasso, L.H. Qu, G. Brugerolle, J.P. Bachellerie, and A. Adoutte. 1988. Partial phylogeny of the unicellular eukaryotes based on rapid sequencing of a portion of 28S ribosomal RNA. *Proc. Natl. Acad. Sci. USA*. 85:3474–3478.

Bartel, P.L., C.T. Chien, R. Sternglanz, and S. Fields. 1993. Using the two-hybrid system to detect protein-protein interactions. *In* Cellular Interactions in Development: A Practical Approach. D.A. Hartley, editor. Oxford University Press, Oxford. 153–179.

Baum, P., C. Furlong, and B. Byers. 1986. Yeast gene required for spindle pole body duplication: homology of its product with Ca2+-binding proteins. *Proc. Natl. Acad. Sci. USA*. 83:5512–5516.

Beranger, F., S. Aresta, J. de Gunzburg, and J. Camonis. 1997. Getting more from the two-hybrid system: N-terminal fusions to LexA are efficient and sensitive baits for two-hybrid studies. *Nucleic Acids Res.* 25:2035–2036.

Bettencourt-Dias, M., and D.M. Glover. 2007. Centrosome biogenesis and function: centrosomics brings new understanding. *Nat. Rev. Mol. Cell Biol.* 8:451–463.

Bobinnec, Y., A. Khodjakov, L.M. Mir, C.L. Rieder, B. Edde, and M. Bornens. 1998. Centriole disassembly in vivo and its effect on centrosome structure and function in vertebrate cells. *J. Cell Biol.* 143:1575–1589.

Bornens, M., and M. Moudjou. 1999. Studying the composition and function of centrosomes in vertebrates. *Methods Cell Biol.* 61:13–34.

Callaini, G., W.G. Whitfield, and M.G. Riparbelli. 1997. Centriole and centrosome dynamics during the embryonic cell cycles that follow the formation of the cellular blastoderm in *Drosophila*. *Exp. Cell Res.* 234:183–190.

Celton-Morizur, S., N. Bordes, V. Fraisier, P.T. Tran, and A. Paoletti. 2004. C-terminal anchoring of mid1p to membranes stabilizes cytokinetic ring position in early mitosis in fission yeast. *Mol. Cell. Biol.* 24:10621–10635.

Chretien, D., B. Buendia, S.D. Fuller, and E. Karsenti. 1997. Reconstruction of the centrosome cycle from cryoelectron micrographs. *J. Struct. Biol.* 120:117–133.

Dutcher, S.K. 2003. Elucidation of basal body and centriole functions in *Chlamydomonas reinhardtii*. *Traffic*. 4:443–451.

Euteneuer, U., R. Graf, E. Kube-Granderath, and M. Schliwa. 1998. *Dictyostelium* gamma-tubulin: molecular characterization and ultrastructural localization. *J. Cell Sci.* 111:405–412.

Fischer, T., S. Rodriguez-Navarro, G. Pereira, A. Racz, E. Schiebel, and E. Hurt. 2004. Yeast centrin Cdc31 is linked to the nuclear mRNA export machinery. *Nat. Cell Biol.* 6:840–848.

Fromont-Racine, M., J.C. Rain, and P. Legrain. 1997. Toward a functional analysis of the yeast genome through exhaustive two-hybrid screens. *Nat. Genet.* 16:277–282.

Geimer, S., and M. Melkonian. 2005. Centrin scaffold in *Chlamydomonas reinhardtii* revealed by immunoelectron microscopy. *Eukaryot. Cell*. 4:1253–1263.

Ishikawa, H., A. Kubo, and S. Tsukita. 2005. Odf2-deficient mother centrioles lack distal/subdistal appendages and the ability to generate primary cilia. *Nat. Cell Biol.* 7:517–524.

Keller, L.C., E.P. Romijn, I. Zamora, J.R. Yates III, and W.F. Marshall. 2005. Proteomic analysis of isolated *Chlamydomonas* centrioles reveals orthologs of ciliary-disease genes. *Curr. Biol.* 15:1090–1098.

Keryer, G., O. Witczak, A. Delouvee, W.A. Kemmner, D. Rouillard, K. Tasken, and M. Bornens. 2003. Dissociating the centrosomal matrix protein AKAP450 from centrioles impairs centriole duplication and cell cycle progression. *Mol. Biol. Cell*. 14:2436–2446.

Kilmartin, J.V. 2003. Sfi1p has conserved centrin-binding sites and an essential function in budding yeast spindle pole body duplication. *J. Cell Biol.* 162:1211–1221.

Kleylein-Sohn, J., J. Westendorf, M. Le Clech, R. Habedanck, Y.D. Stierhof, and E.A. Nigg. 2007. Plk4-induced centriole biogenesis in human cells. *Dev. Cell*. 13:190–202.

Klink, V.P., and S.M. Wolniak. 2001. Centrin is necessary for the formation of the motile apparatus in spermatids of Marsilea. *Mol. Biol. Cell*. 12:761–776.

Koblenz, B., J. Schoppmeier, A. Grunow, and K.F. Lechtreck. 2003. Centrin deficiency in *Chlamydomonas* causes defects in basal body replication, segregation and maturation. *J. Cell Sci.* 116:2635–2646.

Kuriyama, R., and G.G. Borisy. 1981. Centriole cycle in Chinese hamster ovary cells as determined by whole-mount electron microscopy. *J. Cell Biol.* 91:814–821.

Laoukili, J., E. Perret, S. Middendorp, O. Houcine, C. Guennou, F. Marano, M. Bornens, and F. Tournier. 2000. Differential expression and cellular distribution of centrin isoforms during human ciliated cell differentiation in vitro. *J. Cell Sci.* 113:1355–1364.

Lemullois, M., G. Fryd-Versavel, and A. Fleury-Aubusson. 2004. Localization of centrins in the hypotrich ciliate *Paraurostyla weissei*. *Protist.* 155:331–346.

Levy, Y.Y., E.Y. Lai, S.P. Remillard, M.B. Heintzelman, and C. Fulton. 1996. Centrin is a conserved protein that forms diverse associations with centrioles and MTOCs in *Naegleria* and other organisms. *Cell Motil. Cytoskeleton*. 33:298–323.

Li, S., A.M. Sandercock, P. Conduit, C.V. Robinson, R.L. Williams, and J.V. Kilmartin. 2006. Structural role of Sfi1p-centrin filaments in budding yeast spindle pole body duplication. *J. Cell Biol.* 173:867–877.

Loncarek, J., P. Hergert, V. Magidson, and A. Khodjakov. 2008. Control of daughter centriole formation by the pericentriolar material. *Nat. Cell Biol.* 10:322–328.

Madeddu, L., C. Klotz, J.P. Le Caer, and J. Beisson. 1996. Characterization of centrin genes in *Paramecium*. *Eur. J. Biochem.* 238:121–128.

Middendorp, S., A. Paoletti, E. Schiebel, and M. Bornens. 1997. Identification of a new mammalian centrin gene, more closely related to *Saccharomyces cerevisiae* CDC31 gene. *Proc. Natl. Acad. Sci. USA*. 94:9141–9146.

Mikule, K., B. Delaval, P. Kaldis, A. Jurcyzk, P. Hergert, and S. Doxsey. 2007. Loss of centrosome integrity induces p38-p53-p21-dependent G1-S arrest. *Nat. Cell Biol.* 9:160–170.

Nishi, R., Y. Okuda, E. Watanabe, T. Mori, S. Iwai, C. Masutani, K. Sugasawa, and F. Hanaoka. 2005. Centrin 2 stimulates nucleotide excision repair by interacting with xeroderma pigmentosum group C protein. *Mol. Cell. Biol.* 25:5664–5674.

Paintrand, M., M. Moudjou, H. Delacroix, and M. Bornens. 1992. Centrosome organization and centriole architecture: their sensitivity to divalent cations. *J. Struct. Biol.* 108:107–128.

Paoletti, A., M. Moudjou, M. Paintrand, J.L. Salisbury, and M. Bornens. 1996. Most of centrin in animal cells is not centrosome-associated and centrosomal centrin is confined to the distal lumen of centrioles. *J. Cell Sci.* 109:3089–3102.

Paoletti, A., N. Bordes, R. Haddad, C.L. Schwartz, F. Chang, and M. Bornens. 2003. Fission yeast cdc31p is a component of the half-bridge and controls SPB duplication. *Mol. Biol. Cell*. 14:2793–2808.

Pelletier, L., E. O'Toole, A. Schwager, A.A. Hyman, and T. Muller-Reichert. 2006. Centriole assembly in *Caenorhabditis elegans*. *Nature*. 444:619–623.

Piasecki, B.P., M. Lavoie, L.W. Tam, P.A. Lefebvre, and C.D. Silflow. 2008. The Uni2 phosphoprotein is a cell cycle regulated component of the basal body maturation pathway in *Chlamydomonas reinhardtii*. *Mol. Biol. Cell*. 19:262–273.

Piel, M., P. Meyer, A. Khodjakov, C.L. Rieder, and M. Bornens. 2000. The respective contributions of the mother and daughter centrioles to centrosome activity and behavior in vertebrate cells. *J. Cell Biol.* 149:317–330.

Rattner, J.B., and S.G. Phillips. 1973. Independence of centriole formation and DNA synthesis. *J. Cell Biol.* 57:359–372.

Rieder, C.L., and G. Cassels. 1999. Correlative light and electron microscopy of mitotic cells in monolayer cultures. *Methods Cell Biol.* 61:297–315.

Robbins, E., and N.K. Gonatas. 1964. The ultrastructure of a mammalian cell during the mitotic cycle. *J. Cell Biol.* 21:429–463.

Robbins, E., G. Jentzsch, and A. Micali. 1968. The centriole cycle in synchronized HeLa cells. *J. Cell Biol.* 36:329–339.

Rousselet, A., U. Euteneuer, N. Bordes, T. Ruiz, G. Hui Bon Hua, and M. Bornens. 2001. Structural and functional effects of hydrostatic pressure on centrosomes from vertebrate cells. *Cell Motil. Cytoskeleton*. 48:262–276.

Ruiz, F., N. Garreau de Loubresse, C. Klotz, J. Beisson, and F. Koll. 2005. Centrin deficiency in *Paramecium* affects the geometry of basal-body duplication. *Curr. Biol.* 15:2097–2106.

Salisbury, J.L., A.T. Baron, and M.A. Sanders. 1988. The centrin-based cytoskeleton of *Chlamydomonas reinhardtii*: distribution in interphase and mitotic cells. *J. Cell Biol.* 107:635–641.

Salisbury, J.L., K.M. Suino, R. Busby, and M. Springett. 2002. Centrin-2 is required for centriole duplication in mammalian cells. *Curr. Biol.* 12:1287–1292.

Sheffield, P., S. Garrard, and Z. Derewenda. 1999. Overcoming expression and purification problems of RhoGDI using a family of "parallel" expression vectors. *Protein Expr. Purif.* 15:34–39.

Slot, J.W., H.J. Geuze, S. Gigengack, G.E. Lienhard, and D.E. James. 1991. Immunolocalization of the insulin regulatable glucose transporter in brown adipose tissue of the rat. *J. Cell Biol.* 113:123–135.

Sluder, G., and C.L. Rieder. 1985. Centriole number and the reproductive capacity of spindle poles. *J. Cell Biol.* 100:887–896.

Srsen, V., N. Gnadt, A. Dammermann, and A. Merdes. 2006. Inhibition of centrosome protein assembly leads to p53-dependent exit from the cell cycle. *J. Cell Biol.* 174:625–630.

Stemm-Wolf, A.J., G. Morgan, T.H. Giddings Jr., E.A. White, R. Marchione, H.B. McDonald, and M. Winey. 2005. Basal body duplication and maintenance require one member of the *Tetrahymena thermophila* centrin gene family. *Mol. Biol. Cell*. 16:3606–3619.

Taddei, A., D. Roche, J.B. Sibarita, B.M. Turner, and G. Almouzni. 1999. Duplication and maintenance of heterochromatin domains. *J. Cell Biol.* 147:1153–1166.

Tsang, W.Y., A. Spektor, D.J. Luciano, V.B. Indjeian, Z. Chen, J.L. Salisbury, I. Sanchez, and B.D. Dynlacht. 2006. CP110 cooperates with two calcium-binding proteins to regulate cytokinesis and genome stability. *Mol. Biol. Cell*. 17:3423–3434.

Uetake, Y., J. Loncarek, J.J. Nordberg, C.N. English, S. La Terra, A. Khodjakov, and G. Sluder. 2007. Cell cycle progression and de novo centriole assembly after centrosomal removal in untransformed human cells. *J. Cell Biol.* 176:173–182.

Vojtek, A.B., and S.M. Hollenberg. 1995. Ras-Raf interaction: two-hybrid analysis. *Methods Enzymol.* 255:331–342.

Vorobjev, I.A., and S. Chentsov Yu. 1982. Centrioles in the cell cycle. I. Epithelial cells. *J. Cell Biol.* 93:938–949.

Wolff, A., B. de Nechaud, D. Chillet, H. Mazarguil, E. Desbruyeres, S. Audebert, B. Edde, F. Gros, and P. Denoulet. 1992. Distribution of glutamylated alpha and beta-tubulin in mouse tissues using a specific monoclonal antibody, GT335. *Eur. J. Cell Biol.* 59:425–432.